

Development of a Smart Selective Laser Melting Process

APPENDICES

Stijn CLIJSTERS

Dissertation presented in partial
fulfillment of the requirements for the
degree of Doctor of Engineering
Science (Phd): Mechanical
Engineering

March 2017

Development of a Smart Selective Laser Melting Process

APPENDICES

Stijn CLIJSTERS

Supervisory Committee:
Prof. dr. ir. H. Hens, chair
Prof. dr. ir. J.-P. Kruth, supervisor
Prof. dr. ir. J. Van Humbeeck
Prof. dr. ir. B. Lauwers
Prof. dr. ir. B. Van Hooreweder
Prof. dr. ir. S. Yang
(University of Southampton)

Dissertation presented in partial fulfillment of the requirements for the degree of Doctor of Engineering Science (Phd): Mechanical Engineering

March 2017

© KU Leuven – Faculty of Engineering Science
Celestijnenlaan 300B box 2420, B-3001 Heverlee (Belgium)

Alle rechten voorbehouden. Niets uit deze uitgave mag worden vermenigvuldigd en/of openbaar gemaakt worden door middel van druk, fotocopie, microfilm, elektronisch of op welke andere wijze ook zonder voorafgaande schriftelijke toestemming van de uitgever.

All rights reserved. No part of the publication may be reproduced in any form by print, photoprint, microfilm or any other means without written permission from the publisher.

Contents

- Contents** **i**

- List of Figures** **iii**

- A Appendix** **1**
 - A.1 Common Layer Interface (.CLI) 1
 - A.2 XY2-100 Protocol 23
 - A.3 Optimization of Scan Strategies in Selective Laser Melting of Aluminum Parts with Downfacing Areas 33
 - A.4 Hatchman 41
 - A.4.1 Hatcher Overview 41
 - A.5 LabVIEW implementations 48

List of Figures

A.1	The graphical user interface of <i>Hatchman</i>	42
A.2	A view on the pop-up window of the settings.	43
A.3	A schematic overview of all the hatch settings of <i>Hatchman</i> . . .	45
A.4	Illustration of some of the different hatch strategies implemented in <i>Hatchman</i>	46
A.5	The graphical user interface to select the scan settings.	47
A.6	A schematic overview of the Skin-Core strategy in <i>Hatchman</i> . .	47
A.7	The implementation of calculation of the eccentricity of the melt pool.	49
A.8	Schematic overview of the <i>Mapping Algorithm</i>	50

Appendix A

Appendix

A.1 Common Layer Interface (.CLI)

COMMON LAYER INTERFACE (CLI)

VERSION 2.0

Introduction

The Common Layer Interface (CLI) is a universal format for the input of geometry data to model fabrication systems based on layer manufacturing technologies (LMT). It is suitable for systems using layer-wise photo-curing of resin, sintering or binding of powder, cutting of sheet material, solidification of molten material, and any other systems which build models on a layer-by-layer basis.

CLI is intended as a simple, efficient and unambiguous format for data input to all LMT-based systems, based on a “2½D” layer representation. It is independent of vendors or fabrication machines, and should require only a simple conversion to the vendor-specific internal data structure of the machine. The obligatory parts of the format are also application independent, while the USERDATA command allows user- or application-specific data to be defined in the header. This flexibility allows the format to be used for a wide range of applications, without loss of important information and without excluding data transfer between different applications. One specific application, medical scan data, is already accommodated with appropriate user data. Others can be added as they are defined.

Comments and suggestions for future versions are welcome, and should be forwarded to one of the contacts named in Appendix A.

1. Definitions and general conventions

1.1. 2¹/₂D-Representation

The geometrical information of the intersection of a 3D-model with a plane is called a slice. The volume between two parallel slices is called a layer. The 2¹/₂D-representation of a model is the sum total of layer-descriptions. The slicing plane is parallel to the xy-plane of a right hand cartesian coordinate system. It is assumed that the building direction is the positive z-axis.

1.2. Layer

A layer is the volume between two parallel slices, and is defined by its thickness, a set of contours and (optionally) hatches.

1.3. Contour

Contours represent the boundaries of solid material within a layer, and are defined by polylines (section 1.4). They are classified as internal and external contours (Fig.1). For correct interpretation each contour must be closed and must not intersect itself or another contour.

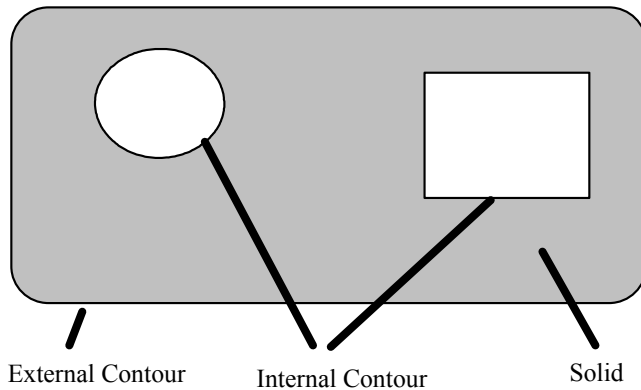


(Fig 1)

1.4. Polyline

A polyline is defined by a set of vertex points (x,y), connected contiguously in the listed order by straight line segments. A closed polyline can also be called a polygon.

1.5. Hatches

A hatch is a set of independent straight lines, each defined by one start and one end point (x,y). The purpose of hatches and open polylines is to define support structures or filling structures to obtain a solid model, which are necessary for some LMT systems.

2. ASCII Data Format

2.1. File Structure

The ASCII-file is separated into sections. Each section is marked by a start and an end marker.

Only the characters A...Z, a...z, , , ., 0...9, \$ and the separators (section 2.4) are interpreted. All other characters will be ignored.

Each file must have a HEADER-section and a GEOMETRY-section. Other sections are optional. The start of the HEADER-section will be interpreted as the start of data, and the end of the GEOMETRY-section as the end of data.

Data may be included before the HEADER-section and after the GEOMETRY-section, but will be ignored.

2.2. General Syntax

All commands have the general form:

Keyword/parameter

Keyword and parameter are separated by the character "/" (oblique stroke). If there are no parameters there should be no oblique stroke. The only exception to this rule is the command "/" (see description below).

2.2.1. Keywords

Keywords are names according to the language description defined below. All keywords are written in ASCII upper case notation. Every keyword must start with the sequence "\$\$".

2.2.2. Parameters

Parameters are numbers or ASCII-strings separated by the character "," (comma).

2.3. Numbers

INTEGER :

$\pm k_1 \dots k_n$: every k_i is a number from 0 to 9.

Negative numbers must have a minus sign, positive numbers can have a plus sign. Numbers with no sign are interpreted as positive. Maximum range is $\pm 2^{31}$.

REAL :

$\pm x_1 \dots x_n.y_1 \dots y_m$

$n \geq 0, m \geq 0$

$l \leq (n + m) \leq \text{realim}$

x_i, y_i are numbers from 0 to 9, respectively before and after the decimal point. Realim is the maximum number of digits within a REAL and is limited to 16. A decimal point is required for all REAL numbers.

2.4. Separators

Separators are "/" (oblique stroke), "," (comma) and "/" (double stroke).

2.5. ASCII-strings

An ASCII-string is any number of valid characters enclosed within double-quotes. Valid characters are all printable characters except the double-quotes.

3. ASCII Language Description

3.1. Non geometric commands

3.1.1. Comments

Command : remark

Syntax : // text //

This is an exception to the general syntax. The text between the // commands will be interpreted as a comment. Within the comment the double stroke is not allowed.

3.1.2. Structure

Command : start header

Syntax : \$\$HEADERSTART

This command starts the HEADER-section, and will be interpreted as the start of data.

Command : end header

Syntax : \$\$HEADEREND

This command ends the HEADER-section.

Command : start geometry

Syntax : \$\$GEOMETRYSTART

This command starts the GEOMETRY-section

Command : end geometry (and end data)

Syntax : \$\$GEOMETRYEND

This command ends the GEOMETRY-section, and will be interpreted as the end of data.

3.1.3. HEADER-Information

Command : data format is binary

Syntax : \$\$BINARY

Indicates the data in the GEOMETRY-section to be binary.

Command : data format is ASCII

Syntax : *\$\$ASCII*

Indicates the data in the GEOMETRY-section to be ASCII.

Command : units are u [mm]

Syntax : *\$\$UNITS/u*

Parameter u : REAL

u indicates the units of the coordinates in mm.

Command : version is v

Syntax : *\$\$VERSION/v*

Parameter v : integer

v divided by 100 gives the version number.

For example 200 --> Version 2.00

All following HEADER-commands are optional.

Command : file was built on date

Syntax : *\$\$DATE/d*

Parameter d : integer

d will be interpreted in the sequence DDMMYY.

Command : dimension

Syntax : *\$\$DIMENSION/x1,y1,z1,x2,y2,z2*

Parameters:

x1, y1, z1, x2, y2, z2 : REAL

Describes the dimensions of the outline box which completely contains the part in absolute coordinates (in mm) with respect to the origin. The conditions $x1 < x2$, $y1 < y2$ and $z1 < z2$ must be satisfied.

Command : number of layers inside the file is i

Syntax : *\$\$LAYERS/i*

Parameter i : INTEGER

The Parameter i indicates the number of layers inside the file.

Command : align data in GEOMETRY-section to 32 bit
(for binary GEOMETRY-section only)

Syntax : *\$\$ALIGN*

Sets the alignment of geometry-data to 32 bit. The command only takes effect in case of a binary GEOMETRY-section. The GEOMETRY-section must start at the beginning of a 32-bit-word. The HEADER-section must end at the end of a 32-bit-word. Every data item within the GEOMETRY-section must start at the beginning of a 32-bit-word. A pair of coordinates (x,y) is seen as one data item. For the commands *start polyline short* and *start hatches short* a pair of coordinates (x,y) are to be written into one 32-bit-word.

Example:

(*\$\$ALIGN* in HEADER-section)

Byte	1	2	3	4	5	6	7	8	9.....
	127	#	#	#	4	1	#	#	129....

Command : set a label for a part

Syntax : *\$\$LABEL/id,text*

Parameter id : INTEGER

text : ASCII-string

id: Identifier to allow more than one model information in one file. For every id used in the commands *start polyline (short/long/ASCII)* and *start hatches (short/long/ASCII)* there shall be one command *\$\$LABEL*. Each id causes the building-process to build a different part.

text: An ASCII string that gives some comment on the part.

Command : put user-specific data to the header

Syntax : *\$\$USERDATA/uid,len,user-data*

Parameters:

uid : ASCII-string

len : long integer

user-data: field of data (binary or ASCII); length is len bytes

uid: user identifier - identifies user and the following user-data.
uid and user-data shall be cleared and published by a central coordinator (e.g. task coordinator).
Example: \$\$USERDATA/"CompanyZZ9401",....

len: defines the length of user-data in bytes from the byte after the comma after the parameter len to the byte before the following \$\$command.

user-data: field of user-specific data; the length of this field is defined by the parameter len; the contents of this field is defined by the user himself.

3.2. Geometric Commands

Command : start layer

Syntax : \$\$LAYER/z

Parameter z : REAL

Start of a layer with upper surface at height z (z*units [mm]). All layers must be sorted in ascending order with respect to z. The thickness of the layer is given by the difference between the z values of the current and previous layers. A thickness for the first (lowest) layer can be specified by including a "zero-layer" with a given z value but with no polyline.

Command : start polyline

Syntax : \$\$POLYLINE/id,dir,n,plx,ply,...pnx,pny

Parameters:

id : INTEGER

dir,n : INTEGER

plx..pny : REAL

id : identifier to allow more than one model information in one file.

id refers to the parameter id of command \$\$LABEL (HEADER-section).

dir : Orientation of the line when viewing in the negative z-direction

0 : clockwise (internal)

1 : counter-clockwise (external)

2 : open line (no solid)

n : number of points

plx..pny : coordinates of the points 1..n

Polylines representing internal contours must be clockwise, polylines representing external contours counter-clockwise (Fig 2). This orientation must be valid for the parameter "dir" and for the order the points are listed. The value of "dir" overwrites the order of listed points if there is a mismatch.

In the case of closed polylines (dir = 0,1) p1x = pnx and p1y = pny must be valid.

The open line value for the dir flag can be used to indicate a non-closed polyline. This can be used as an input for correction and editing tools based on the CLI format.

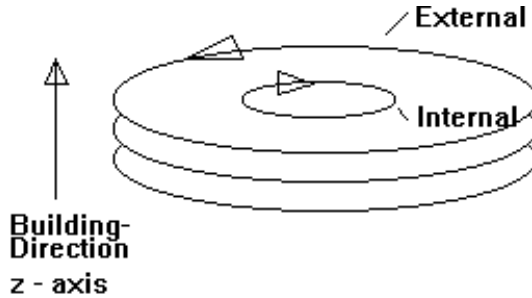


Fig 2

Command : start hatches

Syntax : $\\$HATCHES/id,n,p1sx,p1sy,p1ex,p1ey,...pnex,pney$

Parameters:

id	: INTEGER
n	: INTEGER
p1sx..pney	: REAL

id : identifier to allow more than one model information in one file.

id refers to the parameter id of command $\\$LABEL$ (HEADER-section).

n : number of hatches ($n*4$ =number of coordinates)

p1sx..pney : coordinates of the hatches 1..n

4 parameters for every hatch (startx,starty,endx,endy)

4. ASCII-Data-File-Example

```
$$HEADERSTART
// This is a example for the use of the Layer Format //
$$ASCII
$$UNITS/1 // all coordinates are given in mm //
// $$UNITS/0.01 // all coordinates are given in units 0.01 mm //
$$DATE/070493 // 7. April 1993 //
$$LAYERS/100 // 100 layers //
$$HEADEREND

$$GEOMETRYSTART // start of GEOMETRY-section//
$$LAYER/5.5 // Layer at height z = 5.5 mm//

$$POLYLINE/0,0,5,1.00,2.02,3.30,3.42,5.23,5.01,1.57,5.6,1.00,2.02
$$HATCHES/0,2,10.2,10.4,12.34,12.5,8.8,9.3,15.7,13.2
$$POLYLINE/0,1,10,1.2,4.01,.....
..
..
$$LAYER/5.6
$$POLYLINE/0,0,200,10.23,12.34,.....
.....
..
..
$$LAYER/15.5
$$POLYLINE/0,0,200,13.23,12.34,.....
.....
..
..
$$GEOMETRYEND
```

5. Binary Data Format

5.1. File structure

The binary-data-file is separated into two sections : a header-section in ASCII data format and a geometry-section in binary data format. For header-section commands see section 3.1.3.

The start of the header-section will be interpreted as start of data.

The end of the geometry-section will be interpreted as the end of data.

The end of the header-section must be indicated by a `$$HEADEREND` command.

The geometry-section must directly follow the header-section (directly after the command `$$HEADEREND`) **without** any kind of information (carriage return, line feed etc.) in between.

5.2. General Binary Syntax

All commands have the following general form:

CommandIndex,p1,p2,...pn

There is **no** separator between Command Index and parameters, nor within the parameter-section.

5.2.1. Command Index (CI)

Command Index is a number (unsigned integer) indicating the command according to the command list below.

5.2.2. Parameters

The parameters p1.. pn are numbers according the specification below.

5.3. Numbers

Numbers are specified using the IEEE standard.

Data Formats	Range	Precision	Representation
Unsigned Integer	10^4	16 Bits	[15...0] (Two's Complement)
Long Integer	$10^{\pm 9}$	32 Bits	[31...0] (Two's Complement)
Real	$10^{\pm 38}$	24 Bits	[31 30..23 22..0] s e f s : sign bit e: Biased Exponent f : Significand

Fig. 3

if $0 < e < 255$ then $v = (-1)^s * 2^{(e-127)} * (1.f)$

if $e=0$ and $f \neq 0$ then $v = (-1)^s * 2^{(-126)} * (0.f)$

if $e=0$ and $f=0$ then $v = (-1)^s * 0$

Where e is the Biased Exponent,
 s is the sign bit,
 f is the significand, and
 v the value.

unsigned INTEGER : 2 Bytes
range 0..65535
precision 16 Bits

long INTEGER : 4 Bytes
range 0..+/- 2^{31}
precision 32 Bits

REAL: 4 Bytes
range $10^{\pm 38}$
precision 24 Bits

most significant Byte = highest addressed Byte.

6. Binary Language Description

6.1. Non-geometric commands

No non-geometric commands are specified in version 2.0.

6.2. Geometric Commands

Command : Start Layer long

CI,z

CI 127

Parameter z : REAL

Start of a layer with upper surface at height z (z*units [mm]). All layers must be sorted in ascending order with respect to z. The thickness of the layer is given by the difference between the z values of the current and previous layers. A thickness for the first (lowest) layer can be specified by including a “zero-layer” with a given z value but no polyline.

Command : Start Layer short

CI,z

CI 128

Parameter z : unsigned INTEGER

Start of a layer with upper surface at height z (z*units [mm]). All layers must be sorted in ascending order with respect to z.

Command : Start PolyLine short *Command* : Start PolyLine

CI,id,dir,n,p1x,p1y,...,pnx,pny

CI 129

Parameters:

id : unsigned INTEGER

dir,n : unsigned INTEGER

p1x..pny : unsigned INTEGER

id : identifier to allow more than one model information in one file.

id refers to the parameter id of command \$\$LABEL (HEADER-section).

dir : orientation of the line when viewing in the negative z-direction

0 : clockwise

1 : counter clockwise

2 : open line

n : number of points

p1x..pny : coordinates of the points 1..n

See also section 3.2 command \$\$POLYLINE and section 3.1.3 command \$\$ALIGN and \$\$ LABEL

Command : Start PolyLine long

CI,id,dir,n,p1x,p1y,...pnx,pny

CI 130

Parameters:

id : long INTEGER

dir,n : long INTEGER

p1x..pny : REAL

id : identifier to allow more than one model information in one file.

id refers to the parameter id of command \$\$LABEL (HEADER-section).

dir : orientation of the line when viewing in the negative z-direction

0 : clockwise

1 : counter clockwise

2 : open line

n : number of points

p1x..pny : coordinates of the points 1..n

See also section 3.2 command \$\$POLYLINE and section 3.1.3 command \$\$ALIGN and \$\$ LABEL.

Command : Start Hatches short

CI,id,n,p1sx,p1sy,...pnex,pney

CI 131

Parameters:

id : unsigned INTEGER

n : unsigned INTEGER

p1sx..pney : unsigned INTEGER

id : identifier to allow more than one model information in one file.

id refers to the parameter id of command \$\$LABEL (HEADER-section).

n : number of hatches ($n*4$ = number of coordinates)

p1sx..pney : coordinates of the hatches 1..n

See also section 3.2 command \$\$POLYLINE and section 3.1.3 command \$\$ALIGN and \$\$ LABEL

Command : Start Hatches longCommand : Start PolyLine

CI,id,n,p1sx,p1sy,...pnex,pney

CI 132

Parameters:

id : long INTEGER

n : long INTEGER

p1sx..pney : REAL

id : identifier to allow more than one model information in one file.

id refers to the parameter id of command \$\$LABEL (HEADER-section).

n : number of hatches ($n*4$ = number of coordinates)

p1sx..pney : coordinates of the hatches 1..n

See also section 3.2 command \$\$POLYLINE and section 3.1.3 command \$\$ALIGN and \$\$ LABEL

Appendix A - Development of the Common Layer Interface (CLI)

Development of the Common Layer Interface (CLI) originated in the Brite-EuRam Project “Rapid Prototyping Techniques”, whose work programme identified the following need:

“Problems with the current STL interface (triangle model) force us to look for a new data format for general LMT-processes, which may only contain cross section information... The section oriented information should be vendor independent.”

Simultaneously, the Brite-EuRam Project “Phidias” was working to establish and make available an interface between medical scan data and layer manufacturing technologies. Cooperation between these two projects, together with comments and contributions from third parties, led to the development of CLI version 2.0.

Further development and dissemination of the CLI is also continuing in cooperation with EARP (the European Action on Rapid Prototyping), an organization of companies and institutions throughout Europe which are actively working with rapid prototyping. The up-to-date version of CLI is (from September 1994) continuously available to Internet users under the World Wide Web, at the address given on the next page. This also provides a forum for Internet users to discuss their use of CLI and make suggestions.

Alternatively, copies of the CLI specification can be obtained from the Brite EuRam project contacts listed.

CLI Development Group

Brite EuRam project BE 5278 “RPT - Development and Integration of Rapid Prototyping Techniques for the Automotive Industry”. Partners:

- BIBA, Germany
- BMW AG, Germany
- Centro Recherche FIAT, Italy
- CRIF, Belgium
- EOS GmbH, Germany
- IKP, Germany
- Mercedes Benz AG, Germany

Brite EuRam project BE 5930 “Phidias - Laser Photopolymerisation Models based on Medical Imaging: a Development Improving the Accuracy of Surgery”. Partners:

- Katholieke Universiteit Leuven, Belgium
- Materialise NV, Belgium
- Siemens Medical Engineering Group, Germany
- Zeneca Ltd, United Kingdom

Contacts

Internet addresses for the CLI specification, the EARP electronic book and other information on rapid prototyping (on the World Wide Web hypertext multi-media system):

<http://www.cs.hut.fi/~ado/rp/rp.html> (Mr Andre Dolenc, Helsinki University)

<http://www.cranfield.ac.uk> (Mr Ron. Jamieson, Cranfield University)

Brite EuRam RPT project:

Dr M. Shellabear
EOS GmbH
Pasinger Str. 2
D-82152 Planegg
Germany

Tel: +49 (89) 899131-0

Fax: +49 (89) 8598402

Brite EuRam PHIDIAS project:

Prof W. Kalender
Siemens AG, UB Med
Postfach 3260
D-91052 Erlangen
Germany

Tel: +49 (9131) 84-7736

Fax: +49 (9131) 84-6365

Appendix B - Header section for medical applications

Introduction

This appendix describes a proposal for a *\$\$USERDATA* header section (see 3.1.3) to be used for medical applications.

The extension of the CLI-Header proposed here describes the absolute minimum of labeling considered necessary for medical applications. The definitions are part of work performed within the Brite-Euram project *Phidias* towards the development of a format for the exchange of segmentation results.

The additions are primarily inserted in order to achieve unambiguous documentation and labeling of the history of the data generation process and of the patient orientation in medical applications. For the actual model building process they can be ignored. The CLI-file generation programm must ensure that if x- and y-coordinates and the positive z-direction are interpreted as righthand system, an anatomically correct model will result!

With respect to the coordinate interpretation the following assumptions common in slice oriented imaging modalities are made:

The "volume"/"model"/"stack of layers" coordinate system is defined as a righthand system with the following properties

- x- and y-axis lie within the image/layer plane with
(x) pointing from left to right
(y) pointing from top to bottom
- The z-axis is orthogonal to the slice/image/layer plane with
(z) pointing into the image plane
- The patient orientation is described by another righthand system defined by three base vectors:

medial-rightlateral	(nose->right ear)	as x-axis
posterior-anterior	(spine->chest)	as y-axis: "FRONT-VECTOR"
caudo-cranial	(foot->head)	as z-axis: "HEAD-VECTOR"

The "cartesian coordinates" of HEAD-VECTOR and FRONT-VECTOR in the layer coordinate system fully specify the patient orientation!

Gantry tilt must be taken into account when converting image matrix coordinates into the layer coordinate system! For the sake of simplicity gantry tilt will be ignored, however, when describing patient orientation (the same effect is caused by putting the patient on a slanted couch).

The following three examples use the definitions

<i>axial</i> :	orthogonal to HEAD-VECTOR
<i>coronal</i> :	orthogonal to FRONT-VECTOR
<i>sagittal</i> :	contains HEAD-VECTOR and FRONT-VECTOR

Example 1: Patient in prone position, axial images reconstructed looking in the cranial direction

HEAD-VECTOR = (0, 0, 1)
FRONT-VECTOR = (0, 1, 0)

Example 2: Coronal reconstructions looking onto the chest of the patient

HEAD-VECTOR = (0, -1, 0)
FRONT-VECTOR = (0, 0, -1)

Example 3: Sagittal reconstructions looking from the right to the left side of the patient

HEAD-VECTOR = (0, -1, 0)
FRONT-VECTOR = (1, 0, 0)

Syntax

The `$$USERDATA` section of the CLI-Header (3.1.3) contains information in ASCII-format of the following form (see also page 11)

```
userdata:          {userdata-item}...{userdata-item}
userdata-item:    keyword=text "/0"  ("/0" = binary zero)
```

The following keywords are possible

institution-id	Institution where primary data were generated
source-id	Additional information specifying the creation of this file, eg. software package and person generating the data set
patient-id	Qualifier uniquely specifying the patient
study-id	Qualifier specifying the type of study performed
examination-date	Date on which examination was performed
slice-thickness	Slice thickness in mm
matrix-size	Size of the image matrix (typically 512)
pixel-size	Size of one pixel in mm
gantry-tilt	Gantry tilt of the examination in degrees
front-vector	vector pointing from "spine to chest" expressed in layer coordinates in the form (x,y,z) (see introduction)
head-vector	vector pointing from "feet to head" expressed in layer coordinates in the form (x,y,z) (see introduction)

Example

institution-id=Orthopedic Hospital University of TestTown
source-id=Siemens 3D package Vx.y interactions by Dr. Bone
patient-id=Egon BadLegs I2389/94 20-Jun-1932
study-id=Custom prosthesis left leg
examination-date=20-Jun-1994
slice-thickness=2
matrix-size=512
pixel-size=0.218
gantry-tilt=-7
front-vector=(0,0,1)
head-vector=(0,1,0)

A.2 XY2-100 Protocol

GENERAL DESCRIPTION	2
Interface to the remote XY Scanning Heads	2
PHYSICAL INTERFACE	2
D-TYPE CONNECTOR PIN CONFIGURATION	3
INTERFACE IMPLEMENTATION	4
Differential Driver spec.	5
TIMING CONFIGURATION OF THE XY2-100 INTERFACE	6
TIMING CONFIGURATION OF THE XY2-100-E INTERFACE	7
Note concerning the extended XY2-100 interface :	7
HEAD STATUS	8
Status information of the XY2-100 interface	9

GENERAL DESCRIPTION

The Serial link interface is used to interface between a Vendor XY Scanning head and the XY2-100 or XY2-100-E transceiver on the customer side.

Interface to the remote XY Scanning heads

In order to send the data to the XY Scanning head , the following interface is used. The design provides

- (i) High reliability of data transfer (good noise rejection)
- (ii) Simple implementation (use of traditional transmission methods)
- (iii) Long distance driving capability more as 30 feet (10m)

PHYSICAL INTERFACE

The connection scheme consists of sets of differential line drivers and receivers whose bandwidth is high enough to permit transmission of the data bit by bit to the head over a length of at least 10 meters up to 100 meters. The connector to the head is a 25 way D-type connector.

Signal description

The following signals control communication to the remote head :

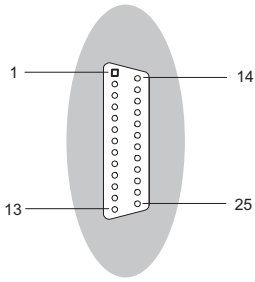
- | | |
|----------------|--------------------------------|
| (i) SENDCK | continuously running clock |
| (ii) SYNC | synchronises the data transfer |
| (iii) CHANNEL1 | data to typically X axis |
| (iv) CHANNEL2 | data to typically Y axis |
| (v) CHANNEL3 | data to typically Z axis |

The following signals allow information to be send back from the remote head.

- | | |
|--------------|---|
| (vi) OPTION2 | used as Position acknowledge Feed back |
| (vii) STATUS | sends the head status
(power/temperature/over position /etc.) back |

D-TYPE CONNECTOR PIN CONFIGURATION

Minimum connection needed for the Serial link

Interface	Pin	Assignment
 <p data-bbox="322 851 527 873">25 Pin D-Sub female connector</p>	1	- SENDCK
	2	- SYNC
	3	- CHANNEL 1
	4	- CHANNEL 2
	5	- CHANNEL 3
	6	- STATUS
	7	reserved for different use
	8	- OPTION2
	9	reserved for different use
	10	reserved for different use
	11	optional Shield ground
	12	reserved for different use
	13	reserved for different use
	14	+ SENDCK
	15	+ SYNC
	16	+ CHANNEL 1
	17	+ CHANNEL 2
	18	+ CHANNEL 3
	19	+ STATUS
	20	reserved for different use
	21	- OPTION2
	22	reserved for different use
	23	optional Shield ground
	24	optional Shield ground
	25	reserved for different use

INTERFACE IMPLEMENTATION

This section deals very briefly with the design implementation of the XY2-100 interface.

The serial link carries the following signals in balanced driver form.

- (i) SENDCK one signal pair (impedance 120 Ohm)
- (i) SYNC one signal pair (impedance 120 Ohm)
- (i) CHANNEL(n) one signal pair (impedance 120 Ohm) for each channel
- (i) STATUS one signal pair (impedance 120 Ohm)

The input commands from the host must be interpreted, reformed and send down the appropriate data channel.

Fig 1 shows the timing of the XY2-100 interface.

Fig 2 shows a timing sample of the XY2-100 interface.

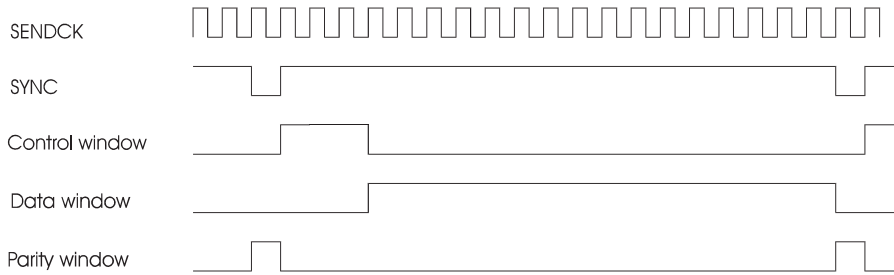


Fig. 1 Timing details of the XY2-100 interface

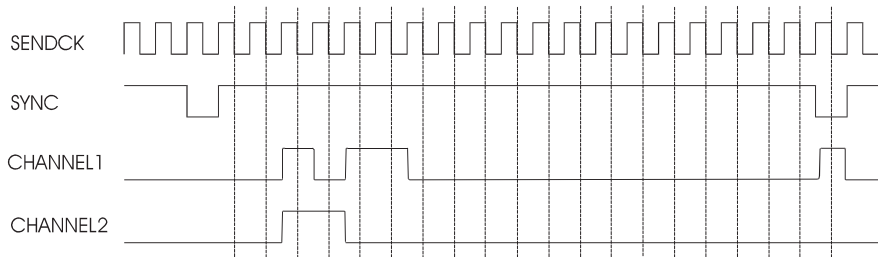
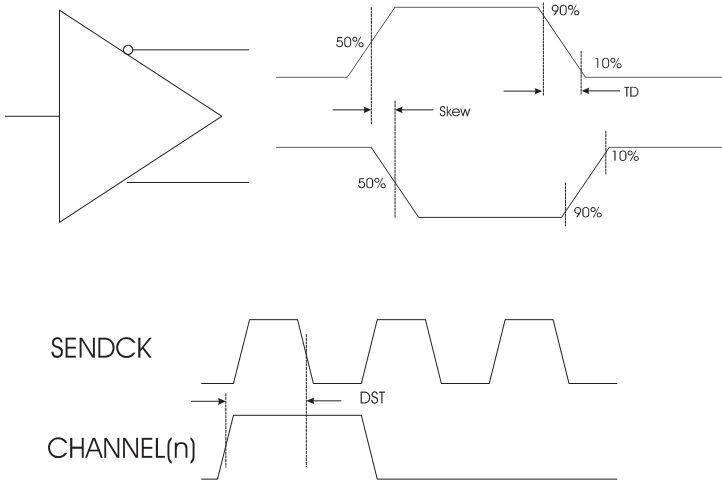


Fig. 2 Timing sample of the XY2-100 interface

Differential Driver spec.



Line driver spec. :

Drive current = min. ± 40 mA

TD differential output delay = max. 15 ns

Skew differential line skew delay = max. 1 ns

SENDCK frequency = 2 MHz

DST SENDCK to CHANNEL(n) set up time

on the driver side = min. 250 ns max. 280 ns

on the receiver side (with cable connected) = min. 250 ns max. 400 ns

TIMING CONFIGURATION OF THE XY2-100 INTERFACE

Table 1:

1	2	3	4	5	6	7	8	9	10	11	12	13	14	15	16	17	18	19	20
CA1	CA2	CA3	MSB	15	14	13	12	11	10	9	8	7	6	5	4	3	2	LSB	par

0	0	1	x	x	x	x	x	x	x	x	x	x	x	x	x	x	x	x	x
---	---	---	---	---	---	---	---	---	---	---	---	---	---	---	---	---	---	---	---



Control code 1 for standard data transfer :

CA1 = 0
CA2 = 0
CA3 = 1

Control code 2 for Serial link data test :

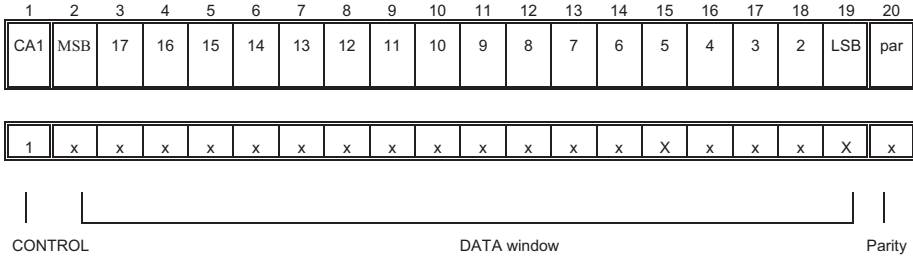
CA1 = 0
CA2 = 1
CA3 = 1

The used parity is a even parity.

The Data window can deliver 16 Bit's data.

TIMING CONFIGURATION OF THE XY2-100-E INTERFACE

Table 2:



Control code for the 18 bit transfer :
 Used on all heads
 CA1 = 1

The used parity is a odd parity.
 The Data window deliver 18 Bit's data.

Note concerning the extended XY2-100 interface :

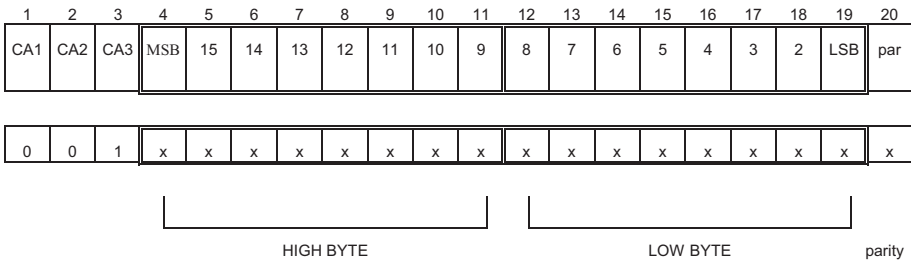
The receiver checks the receiving data from the Serial link and automatically adjust itself to the used Serial link standard .
 The data transfer between receiver and DAC's is automatically adjusted to the used DAC .
 The used DAC's on the receiver is a 18 bit's version.

HEAD STATUS

Note: Status output not supported on all models!

The Head status is the received data through the Serial link.
There are 2 different selection codes available with active parity.

Table 3:



selection code 1 CKST :

CA1 = 0
CA2 = 0
CA3 = 1

selection code 2 CKEDD :

CA1 = 0
CA2 = 1
CA3 = 1

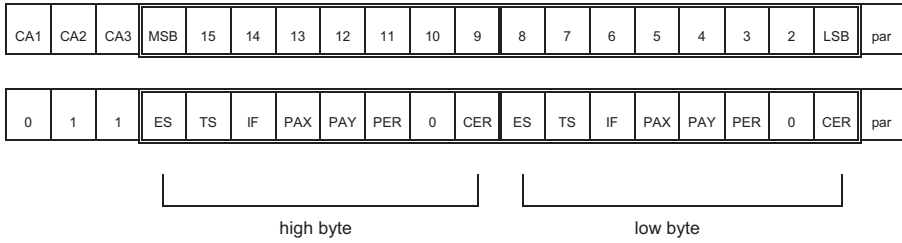
Set the desired selection code on the transceiver to receive the status from the head.

for CKST or CKEDD

Status information of the XY2-100 interface

Table 4:

The status is read in as a 16 bit word whereas only the high byte MSB to bit 9 are used for the status information.



ES = Error Status including Power, Scanner AGC, Over position

TS = Temperature Status

IF = Infield status (not used fix assigned to level 1)

PAX = Position acknowledge X axis

PAY = Position acknowledge Y axis

PER = Parity error

CER = Clock error

1* = OK

1* = OK

1 = OK

1 = within window

1 = within window

1 = no error

1 = no error

- * these bits are AND-gated X&Y flags.

A.3 Optimization of Scan Strategies in Selective Laser Melting of Aluminum Parts with Downfacing Areas

Raya Mertens¹

Division of Production Engineering,
Machine Design and Automation,
Department of Mechanical Engineering,
University of Leuven (KU Leuven),
Leuven 3001, Belgium
e-mail: raya.mertens@kuleuven.be

Stijn Clijsters

Division of Production Engineering,
Machine Design and Automation,
Department of Mechanical Engineering,
University of Leuven (KU Leuven),
Leuven 3001, Belgium
e-mail: stijn.clijsters@kuleuven.be

Karolien Kempen

Division of Production Engineering,
Machine Design and Automation,
Department of Mechanical Engineering,
University of Leuven (KU Leuven),
Leuven 3001, Belgium
e-mail: karolien.kempen@kuleuven.be

Jean-Pierre Kruth

Division of Production Engineering,
Machine Design and Automation,
Department of Mechanical Engineering,
University of Leuven (KU Leuven),
Leuven 3001, Belgium
e-mail: jean-pierre.kruth@kuleuven.be

Optimization of Scan Strategies in Selective Laser Melting of Aluminum Parts With Downfacing Areas

Selective laser melting (SLM) is an additive manufacturing technique in which metal products are manufactured in a layer-by-layer manner. One of the main advantages of SLM is the large geometrical design freedom. Because of the layered build, parts with inner cavities can be produced. However, complex structures, such as downfacing areas, influence the process behavior significantly. The downfacing areas can be either horizontal or inclined structures. The first part of this work describes the process parameter optimization for noncomplex, upfacing structures to obtain relative densities above 99%. In the second part of this research, parameters are optimized for downfacing areas, both horizontal and inclined. The experimental results are compared to simulations of a thermal model, which calculates the melt pool dimensions based on the material properties (such as thermal conductivity) and process parameters (such as laser power and scan speed). The simulations show a great similarity between the thermal model and the actual process. [DOI: 10.1115/1.4028620]

Keywords: SLM, AISi10Mg, downfacing structures

1 Introduction

SLM is a production technique that builds products in a layer-by-layer fashion. Figure 1 shows a schematic overview of the process. For each part-layer to be produced, a layer of powder, with a typical layer thickness of 30 μm , is deposited on the build platform. Subsequently, the laser scans predefined areas and melts the powder locally. Once the scanning is finished, the build platform moves down and the cycle repeats until the part is completed.

The use of different parameters determines the nature of the process. The scan strategy consists of two parts, namely, the scan parameters or parameter set (laser power, scan speed, scan spacing, and layer thickness) and the scan pattern (laser path).

The first requirement in the production of qualitative SLM parts consists of obtaining nearly fully dense parts [1,2]. To fulfill this requirement, the parameter set has to be optimized. This parameter set is used to produce parts without downfacing areas. Density optimization of aluminum is investigated before in Refs. [3] and [4].

A second requirement arises when parts with downfacing areas are produced. Such downfacing areas are often encountered in complex products with, for example, internal cooling channels. These areas need an adapted scan strategy. In these areas, the laser scans on top of several layers of unmolten powder, which changes the melting behavior. Optimizing the downfacing scan strategy enables the production of qualitative complex parts, thus

enlarging the geometrical freedom and the number of applications of the SLM process.

Scan strategy optimization for downfacing areas is previously investigated in Ref. [5] for horizontal structures and in Ref. [6] for inclined structures. This research uses a strategy that is based on Ref. [5] to be able to produce horizontal downfacing areas.

2 Procedure

2.1 Equipment. The SLM machine used in this research is an in-house built machine of KU Leuven—PMA. Table 1 summarizes the properties of the optical setup. All parts were built in an Ar atmosphere.

2.2 Material. In this research, the scan strategy is optimized for AISi10Mg. This aluminum alloy is a casting-alloy. Previous research [3,4] shows that AISi10Mg is an alloy that is suitable for SLM, due to its high amount of silicon that improves the alloy's "fluid life."

The chemical composition of this alloy is presented in Table 2. The two most important alloying elements are silicon and magnesium. Silicon has limited solubility and yet undergoes a relatively large volume fraction of isothermal solidification, thus gaining significant strength while undergoing little or no thermal

Table 1 Laser properties of the in-house built SLM machine

Type	Yb fiber laser
Maximal power (P)	300 W
Wavelength (λ)	1064 nm
Spot diameter ($d_{99\%}$)	80 μm

¹Corresponding author.

Contributed by the Manufacturing Engineering Division of ASME for publication in the JOURNAL OF MANUFACTURING SCIENCE AND ENGINEERING. Manuscript received April 15, 2014; final manuscript received September 9, 2014; published online October 24, 2014. Assoc. Editor: Darrell Wallace.

Table 2 Chemical composition of AISi10Mg (ISO 3522)

Weight percentage	Al	Si	Fe	Cu	Mn	Mg	Zn	Ti	Others
	86.9–90.8	9.0–11.0	≤0.55	≤0.10	≤0.45	0.20–0.45	≤0.10	≤0.15	≤0.30

contraction. This is very important to avoid hot cracking issues. Magnesium’s role is to strengthen and harden the aluminum alloy. Silicon combines with magnesium to form the hardening Mg₂Si phase.

2.3 Parameter Optimization. In the first step of this research, the scan parameters are optimized in terms of density. After this optimization, simple geometries with nearly full-density can be produced.

In a second step, downfacing structures (both horizontal and inclined) are considered. They require an adapted scan strategy to avoid dross formation or collapsing downfacing surfaces (Fig. 2).

2.3.1 Density Optimization for Cubic Parts. In order to produce fully dense parts, the scan parameters (laser power, scan speed, scan spacing, and layer thickness) have to be carefully optimized [7–9]. In this research, laser power and scan speed are varied, while the scan spacing and layer thickness are kept constant at, respectively, 105 μm and 30 μm. These parameters were determined in initial research on SLM of AISi10Mg [3], and this research shows that they are also applicable here.

In the scan pattern that was used, the laser tracks within one layer are parallel but have alternating directions (zig-zag). This pattern is rotated over 90 deg for consecutive layers.

The relative density of the parts is measured by Archimedes’ principle. The samples are weighted both in air and in ethanol. Based on the difference in weight and the density of ethanol, density values are calculated. Dividing these values by the theoretical value of the material results in relative density values. Besides Archimedes, optical microscope images are used to verify the size, morphology, and distribution of the pores.

2.3.2 Downfacing Structures. Downfacing structures need an adapted scan strategy. Because downfacing areas are scanned on multiple layers of loose powder (instead of on solidified material), their melt pool behavior is different. Due to the lower (and non-uniform) heat-conductivity of the powder, the melt pool becomes very unstable and deep if the scan strategy is not optimized, resulting in random dross formation (Fig. 2).

The parameter optimization is based on simulations of a thermal model and on experimental tests. The thermal model is developed within the University of Leuven (KU Leuven). The model is based on an enthalpy formulation [Eq. (1)], which is nonlinear due to the relation between temperature and enthalpy. Enthalpy values of the material are calculated numerically by using explicit forward Euler time integration and central differencing for the

space derivatives. The aggregation states of the material are then obtained based on these enthalpy values [10].

The experimental tests focus on the density of the entire part and of the downfacing layers in particular, geometrical accuracy and surface quality. Evaluation is mainly based on microscope images and visual inspection

$$\frac{\partial H}{\partial t} = \nabla \cdot k \nabla T + S_V + S_S \quad (1)$$

where H is enthalpy, T is temperature, t is time, S_V is volume source term, k is thermal conductivity, and S_S is surface source term.

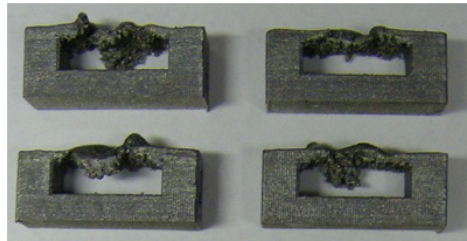


Fig. 2 Dross formation due to deep unstable melt pool in downfacing areas with a length of 10 mm

Figure 3(a) shows the geometry and dimensions of the produced parts, containing downfacing areas.

Besides horizontal downfacing structures, inclined structures are also taken under investigation (Fig. 3(b)). To check the angles of the produced parts, a vision measuring system (Quick Vision Pro 202) is used [11]. On these images, the upfacing and downfacing edges of the part cavity are fitted by lines through a minimum of 60 points and the angle between these two edge lines is measured.

3 Results and Discussion

3.1 Density Optimization for Cubic Parts. Figure 4 shows the relative densities achieved for each combination of laser power and scan speed. For aluminum alloys in general, the use of high powers results in high densities. Therefore, the power is varied between 240 W and 300 W, which is the maximum power of the laser. The scan speed is varied in a way that densities higher than 99% are achieved, without using scan speeds that are too low in order to guarantee the productivity of the process.

In this parameter range, densities increase when power increases or scan speed decreases. Hence, the density increases when the energy input increases. This energy input is presented by Eq. (2). Relative densities are higher than 99% when ϕ is larger than 0.2 Ws/mm.

$$\phi = \frac{P}{v} \quad (2)$$

The optimal parameter set in terms of part density consists of a laser power of 300 W and a scan speed of 1400 mm/s. A high power is preferable because it allows a higher scan speed and therefore a high productivity. The relative density based on five parts is 99.3%±0.2% (95% confidence interval).

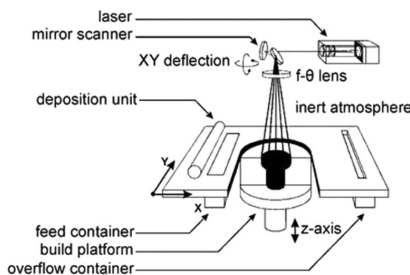


Fig. 1 Schematic overview of the SLM process

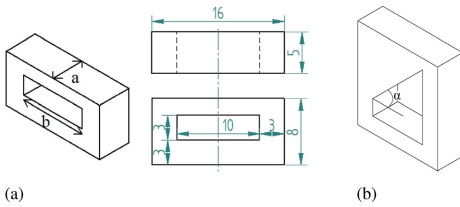


Fig. 3 Downfacing structures. (a) Horizontal and (b) Inclined.

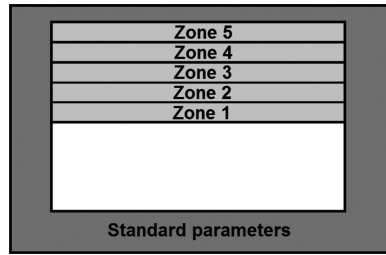


Fig. 6 Different zones of a downfacing structure

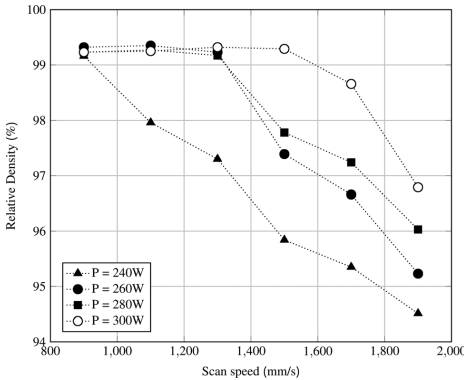


Fig. 4 Relative density in function of scan speed and laser power

These high densities are confirmed using light optical microscopy. Figure 5 shows a top view and a side view of an SLM-cube. There are still pores present in the workpiece, but they are very small, and the number of pores is limited. The pores are mainly situated near the borders of the piece.

3.2 Downfacing Structures. Research on downfacing structures is divided into three parts: horizontal downfacing structures, extended or large horizontal downfacing structures, and inclined structures.

3.2.1 Horizontal Downfacing Structures. Previous research on downfacing areas in Ti6Al4V [5] indicates the successful use of different parameter zones above the downfacing area (Fig. 6). This strategy is also used in this work.

The area above the downfacing surface is divided into five zones. These zones each consists of multiple layers and they all have an adapted parameter set. In this way, a gradual transition to

the standard parameters (parameters to obtain optimal density) of 300 W and 1400 mm/s can be accomplished.

To find an optimal parameter set for the five adapted zones, first a parameter set for the first zone has to be estimated. Parameters for the following zones are obtained by making a smooth transition from zone 1 to standard parameters.

The optimal parameter set for the first downfacing zone is determined based on simulations on one side, and on experimental tests on the other side.

Two scanning parameters have to be optimized: laser power (P) and scan spacing (h). To guarantee an acceptable productivity, scan speed (v) is kept constant at 1400 mm/s.

Thermal model. Simulations are performed both for a normal scanning situation (Fig. 7(a)) and a downfacing scanning situation (Fig. 7(b)). In the normal scanning situation, the laser scans one layer of powder (represented by the top 30 μm in the figure) on top of a solid base. The melt pool is also visible in the simulation. This simulation uses a power of 300 W and scan speed of 1400 mm/s as was found to be the optimal parameter set for normal, upfacing scanning situations.

In the downfacing scanning situation (Fig. 7(b)), the downfacing geometry is simulated. The left pillar is shown between 0 and 120 μm along the x -axis. After 120 μm , the volume is filled with powder. Here, three different powers of 20 W, 60 W, and 300 W are used.

Because only single-tracks are simulated, no conclusions can be drawn about the scan spacing.

From Fig. 7(b), it is clear that the melt pool enlarges with increasing power. To insure a stable melt pool, the melt pool dimensions cannot be too small, nor too large in order to avoid irregularities or droplets [3]. The melt pool dimensions can be evaluated by comparing them to the melt pool dimensions of the normal scanning situation, because the experimental tests showed that this corresponds to a stable melting situation. Melt pool width and depth of the 60 W downfacing situation is similar to the dimensions of the normal scanning situation (width of 125 μm and depth of 60 μm). A power of 20 W results in a melt pool that is too small; a power of 300 W (which is used for the normal scanning situation) results in a very large melt pool. This is due to the lower heat

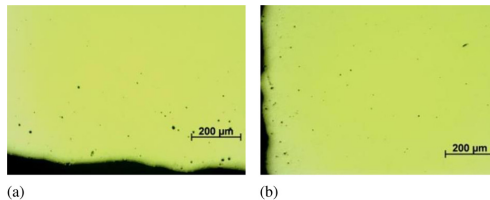


Fig. 5 Microscope images show high density of 99.3%. (a) Top view and (b) Side view.

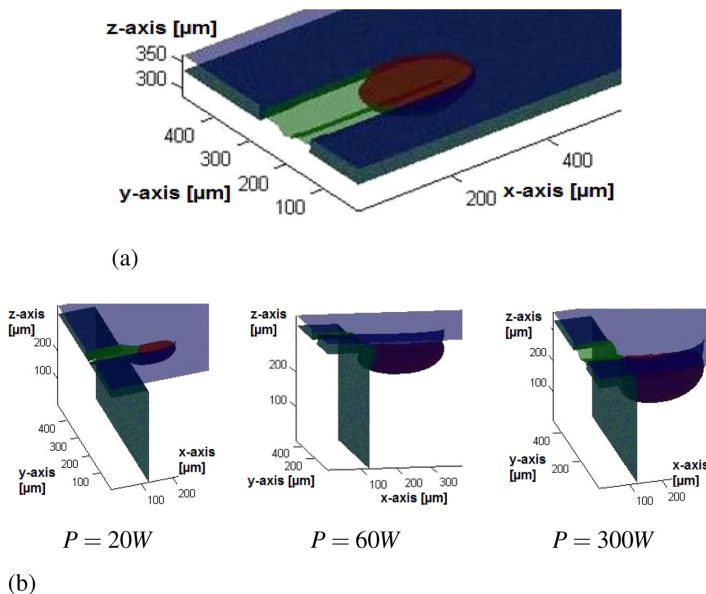


Fig. 7 Simulation results. (a) Normal scanning situation on solidified material and (b) Down-facing scanning situation.

conductivity of the powder material in comparison to solid material.

Based on the thermal model, a laser power of approximately 60 W results in a stable process.

Experimental tests. In these tests, first the effect of the scan spacing is investigated. Reducing the scan spacing results first in smoother surfaces until it reaches an optimal value. Further reducing the scan spacing then leads to rougher surfaces. An optimal scan spacing is found to be 20 μm .

To determine the optimal laser power, several parts with different laser powers of zone 1 are produced and compared. Figure 8 gives an overview. The power is varied between 40 W and 90 W. Outside of these values, the production fails due to curling up of the downfacing layers.

When the power of the first zone is too low, no powder is melted. On the other hand, when power is too high, large irregular lumps are formed. These lumps lower the surface quality and can cause problems in post-treatments like sandblasting or etching. These lumps are also visible to the naked eye. Figure 9 compares downfacing surfaces scanned with laser powers of 35 W and 85 W. In the image of 85 W, larger lumps are visible. The conclusion here is that there is a relative large range of applicable powers, but the results show large differences. A power of 60 W insures that in the first downfacing layers some powder is already molten while avoiding large lump formation.

Results. Both simulations and tests indicate a power of 60 W to be used for the first zone of the downfacing structure. According to the experimental tests, a scan spacing of 20 μm is recommended.

Now that the parameters for the first zone are determined, parameters for the next zones are obtained by making the smooth transition to standard parameters.

The optimal scan strategy for horizontal downfacing structures is displayed in Table 3. From this table, it is clear that the power increases every zone. Because of the increase in power, the scan spacing has to be larger for zone 2 in comparison to zone 1.

Every zone requires ten layers to obtain a stable process.

Figure 10 shows the produced downfacing structures.

Figure 11 shows a cross section that is taken perpendicular to the image of Fig. 10. It is clear that there is warp present toward the front and the back of the structure. The warp is a result of thermal stresses that are present in the SLM-pieces. On the borders of the downfacing structure, there is no mechanical support. This also implies that there is no heat sink present at these borders which complicates the heat dissipation. This results in curling only at these location. Figure 11 shows that the sides only have a thickness of about ten layers (300 μm) instead of the designed 60 layers (1800 μm).

3.2.2 Extended/Larger Downfacing Structures. When producing larger downfacing areas, results are influenced by the heat transport situation [12]. In a small downfacing area, the main direction in which heat is conducted points from the middle of the downfacing structure to the sides as shown in Fig. 12.

In wide downfacing structures (the width is presented by a in Fig. 3), this situation does not change. The path the heat has to travel still has the same length. That is why wide downfacing structures can easily be produced using the scan strategy from Table 3. Figure 13 demonstrates this. Here, a downfacing structure with a width of 40 mm is produced.

Problems however, arise when long downfacing structures are produced (the length is presented by b in Fig. 3). The path from the middle of the downfacing structure to the sides becomes longer and without extra measures, the downfacing structure will fail.

The geometry of Fig. 14(a) offers a solution for this problem. In this geometry, extra supports are placed at the edges of the downfacing structure. These supports provide extra channels for heat transport. They also give more mechanical support to the downfacing structure. The result of this geometry scanned with the strategy from Table 3 is displayed in Fig. 14(b).

3.2.3 Inclined Structures. Because of the less extreme situation, the adapted strategy for inclined downfacing structures is limited to only three zones before using standard parameters.

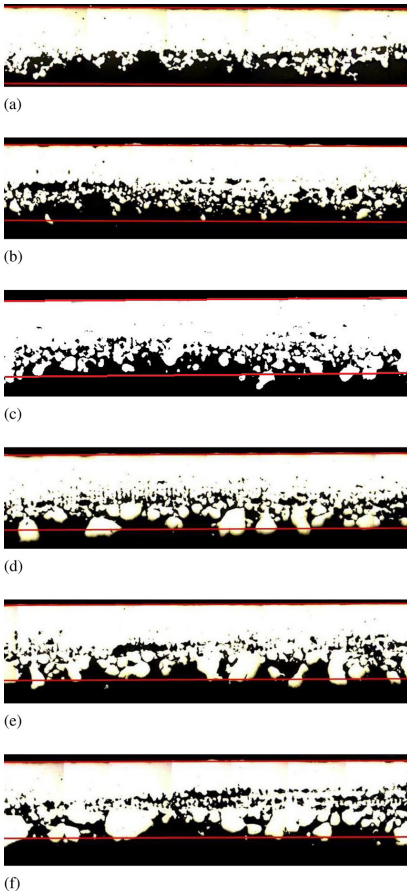


Fig. 8 Comparison of the different powers used in zone 1. The lines indicate the borders of a perfect downfacing area. The length of the pieces is 10 mm. (a) 40 W, (b) 50 W, (c) 60 W, (d) 70 W, (e) 80 W, and (f) 90 W.

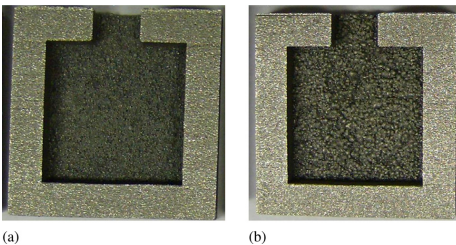


Fig. 9 Comparison of two downfacing areas of 14 mm x 14 mm. When using high powers, large lumps are formed. (a) 35 W and (b) 85 W.

Table 3 Optimal parameter set for downfacing structures in AISi10Mg ($v = 1400$ mm/s)

	Z1	Z2	Z3	Z4	Z5	Standard parameters
Laser power (W)	60	90	120	150	220	300
Scan spacing (μm)	20	110	110	110	110	110
Number of layers	10	10	10	10	10	Rest (here 10)

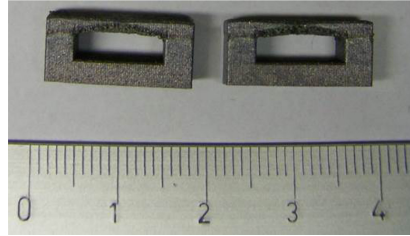


Fig. 10 Picture of a downfacing structure with a length of 10 mm



Fig. 11 Warp of the downfacing structure



Fig. 12 Heat transport situation in downfacing structures

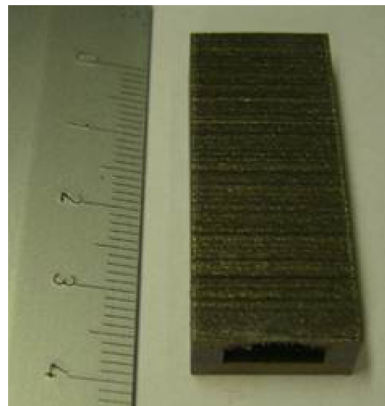


Fig. 13 Wide downfacing structure of 40 mm

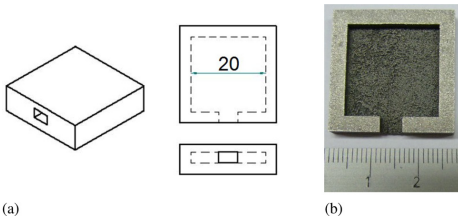


Fig. 14 Adapted geometry to obtain longer downfacing structures with a length of 20 mm. (a) Geometry and (b) Result.

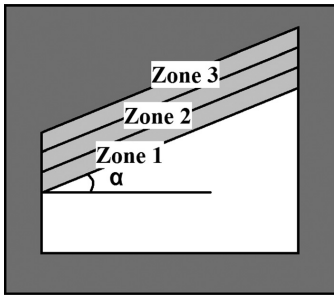


Fig. 15 Different zones of an inclined area with angle α

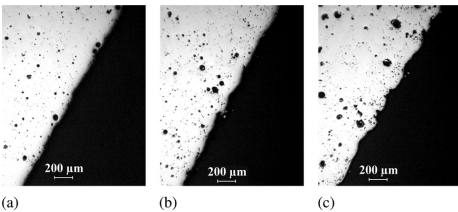


Fig. 16 Microscope images of inclined structures ($\alpha = 60$ deg) with different power used in zone 1. (a) 100 W, (b) 200 W, and (c) 300 W.

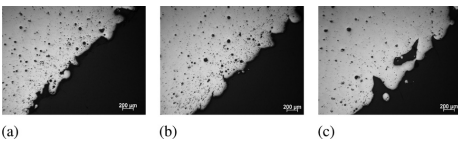


Fig. 17 Microscope images of inclined structures ($\alpha = 45$ deg) with different power used in zone 1. (a) 100 W, (b) 200 W, and (c) 300 W.

Table 4 Scan strategy for inclined structures with an angle of 30 deg

	Zone 1	Zone 2	Zone 3	Standard parameters
Power (W)	120	150	180	300
Number of layers	15	15	15	Rest

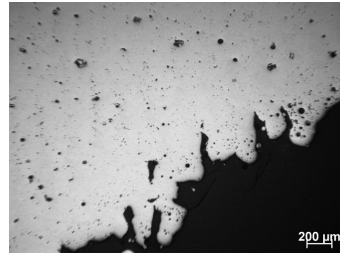


Fig. 18 Microscope image of the inclined structure of 30 deg

Figure 15 illustrates this strategy. In this strategy, each zone uses the same scan spacing of $110 \mu\text{m}$. Parameters are optimized for three inclination angles, namely 60 deg, 45 deg, and 30 deg. These angles are defined as shown in Fig. 15.

Inclined angle of 60 deg. Structures with an inclined angle of 60 deg can be produced with a laser power of 300 W in all zones. The result of such a structure is shown in Fig. 18. The angle of this piece measured by the vision measuring system has a 95% confidence interval of $60.14 \text{ deg} \pm 0.09 \text{ deg}$ based on five measurements of the same piece.

Though standard parameters can be used in zone 1, it is interesting to look at the influence of the power on the surface quality of the structure. Therefore, different samples are made with each time a different power of the first zone of the inclined structure. Figure 16 shows microscope images of these pieces.

From this figure, it is clear that power affects surface quality. Lower powers result in smoother surfaces whereas larger powers lead to less smooth downfacing surfaces.

Inclined angle of 45 deg. A structure with an inclination angle of 45 deg can also be produced with a power of 300 W (Fig. 18). The 95% confidence interval of the angle is $45.07 \text{ deg} \pm 0.48 \text{ deg}$ based on five measurements of this inclined structure.

In analogy to the 60 deg. inclination angle, the influence of the power used in the first zone on the surface quality is investigated.

Figure 17 gives an overview of the microscope images. First of all, these surfaces are much less smooth than the surfaces that have an inclined angle of 60 deg. This confirms the expectations since this downfacing structure is a little more extreme. This rough surface also explains the larger confidence interval of the measured angle compared to the 60 deg. angle. Further, the differences in surface quality for different powers are less significant for this angle.

Inclined angle of 30 deg. An inclined structure of 30 deg cannot be produced by using only high powers. For this case, the strategy of Table 4 is used.

Figure 18(c) displays this structure. The microscope image is shown in Fig. 19. The surface of this piece is very rough.

The angle of this inclined structure is again measured by the vision measuring system. The 95% confidence interval based on five measurements is $31.44 \text{ deg} \pm 0.68 \text{ deg}$. The angle is clearly

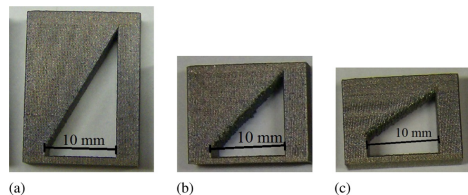


Fig. 19 Parts produced with inclined structures. (a) 60 deg, (b) 45 deg, and (c) 30 deg.

too large. This indicates that there is warp present due to thermal stresses. During the production of each layer, the end of the piece curls up a little further. Because of the limited size of the inclined structure, the warp did not cause problems during production. When the downfacing length increases, problems concerning the deposition unit are to be expected. (The curled up part blocks the deposition unit when placing a new layer of powder.)

4 Conclusion

In this research, scan strategies are optimized for AlSi10Mg.

First of all, the strategy to obtain high densities for upfacing structures is investigated. The combination of a power of 300 W and scan speed of 1400 mm/s results in relative densities of $99,3\% \pm 0,2\%$ (95% confidence interval).

Subsequently, scan strategy for downfacing structures are obtained. The scan pattern used is based on a scan pattern developed in Ref. [5]. Scan parameters are obtained based on simulations of a thermal model and on experimental tests. Simulations of a downfacing scanning situation using different parameters are compared to a simulation of a normal scanning situation. A downfacing power of 60 W results in similar melt pool dimensions compared to the normal scanning situation. Experimental tests show that no powder is melted when laser powers are too low. On the other hand, when laser powers are too high, lumps are formed.

Table 3 summarizes the scan strategy for downfacing structures.

Larger downfacing areas can be produced by using the parameter set of Table 3, but there are limitations. Long downfacing structures need extra supports on both sides to provide mechanical resistance and extra heat transport channels.

Finally, inclined structures are examined. When the angle between the inclined downfacing surface and a horizontal line is large enough, high powers can be used. Though, these high powers can be negative for surface quality. The research shows that low powers give better surface quality for an inclination angle of 60 deg.

For small angles, an adapted scan strategy is needed to prevent warp of the structure. Results show that even with this adapted strategy, some warp is present due to thermal stresses.

Acknowledgment

The research leading to these results has received funding from the European Union's Seventh Framework Programme (FP7/2007-2013) under Grant Agreement No. 314055.

References

- [1] Edwards, P., O'Connor, A., and Ramulu, M., 2013, "Electron Beam Additive Manufacturing of Titanium Components: Properties and Performance," *ASME J. Manuf. Sci. Eng.*, **135**(6), p. 061016.
- [2] Mahamood, R., Akinlabi, E., Shukla, M., and Pityana, S., 2013, "Characterizing the Effect of Laser Power Density on Microstructure, Microhardness, and Surface Finish of Laser Deposited Titanium Alloys," *ASME J. Manuf. Sci. Eng.*, **135**(6), p. 064502.
- [3] Kempen, K., Thijs, L., Yasa, E., Badrossamay, M., Verhecke, W., and Kruth, J.-P., 2011, "Process Optimization and Microstructural Analysis for Selective Laser Melting of AlSi10Mg," *Solid Freeform Fabrication Symposium*, **22**(2011), pp. 484–495.
- [4] Kempen, K., Thijs, L., Van Humbeeck, J., and Kruth, J.-P., 2012, "Mechanical Properties of AlSi10Mg Produced by Selective Laser Melting," *Phys. Procedia*, **39**, pp. 439–446.
- [5] Clijsters, S., Craeghs, T., and Kruth, J.-P., 2012, "A Priori Parameter Adjustment for SLM Process Optimization," *Innovative Developments in Virtual and Physical Prototyping*, Taylor & Francis Group, New York, pp. 553–560.
- [6] Wang, D., Yang, Y., Yi, Z., and Su, X., 2012, "Research on the Fabricating Quality Optimization of the Overhanging Surface in SLM Process," *Int. J. Adv. Manuf. Technol.* **65**(9–12), pp. 1471–1484.
- [7] Mumtaz, K. A., Erasenthiran, P., and Hopkinson, N., 2008, "High Density Selective Laser Melting of Waspaloy[®]," *J. Mater. Process. Technol.*, **195**(1–3), pp. 77–87.
- [8] Buchbinder, D., Schleifenbaum, H., Heidrich, S., Meiners, W., and Bültmann, J., 2011, "High Power Selective Laser Melting (HP SLM) of Aluminum Parts," *Phys. Procedia*, **12**(2011), pp. 271–278.
- [9] Vrancken, B., Thijs, L., Kruth, J.-P., and Van Humbeeck, J., 2012, "Heat Treatment of Ti6Al4V Produced by Selective Laser Melting: Microstructure and Mechanical Properties," *J. Alloys Compd.*, **541**, pp. 177–185.
- [10] Verhaeghe, F., Craeghs, T., Heulens, J., and Pandelaers, L., 2009, "A Pragmatic Model for Selective Laser Melting With Evaporation," *Acta Mater.* **57**(20), pp. 6006–6012.
- [11] Mitutoyo American Corporation, 2013, <http://catalog.mitutoyo.com/Vision-Measuring-Systems-C102.aspx>
- [12] Paul, R., Anand, S., and Gerner, F., 2014, "Effect of Thermal Deformation on Part Errors in Metal Powder Based Additive Manufacturing Processes," *ASME J. Manuf. Sci. Eng.*, **136**(3), p. 031009.

A.4 Hatchman

A.4.1 Hatcher Overview

An overview of *Hatchman* is given here to have a summary of the software. This appendix can also be used as a tutorial of *Hatchman*. This overview is build up as the program graphical interface (*figure A.1*). All the steps have to be executed in the order listed below to complete the hatching successfully. Below is a small walkthrough to illustrate how the buttons work and their functions.

- 1. Select file:** The .CLI file of the part that needs to be hatched, coming from the slicing tool (e.g. Magics) is selected.
- 2. Convert and fix file:** This step will check the .CLI file for errors and transfer it in an easy to read and acces file for the hatcher.
- 3. Load converted file:** Before the real hatching can start, all the fixed layers containing the contours are loaded into the memory.
- 4a. Select hatch settings:** This settings button will pop up a new menu box where most of all the hatch settings can be defined. Settings that can be selected for example are hatching pattern, track distance and island size. More details about the possible settings are given in the next subsections.
- 4b. Scan settings:** This button will pop up another settings window, focusing on the different types of vectors in the tool path. This window allows to give each different vector class a different ID. The detailed explanation of these scan settings will follow in the next subsections
- 5. Perform calculation:** Once all the settings are selected and the file is loaded the generation of the tool path can be triggered by this command. A sequence of algorithms are used sequently, to detect different features as thin walls, downfacing areas or other and to fill the contours with a laser tool path out of different vectors. The algorithms and output are explained more into detail later in this chapter.
- 6. Vector check:** In a last step before storing the tool path to a file the tool path has a final check to eliminate needless movements.
- 7. Save in file:** This button will initiate the saving of the hatched part into an .STS file.

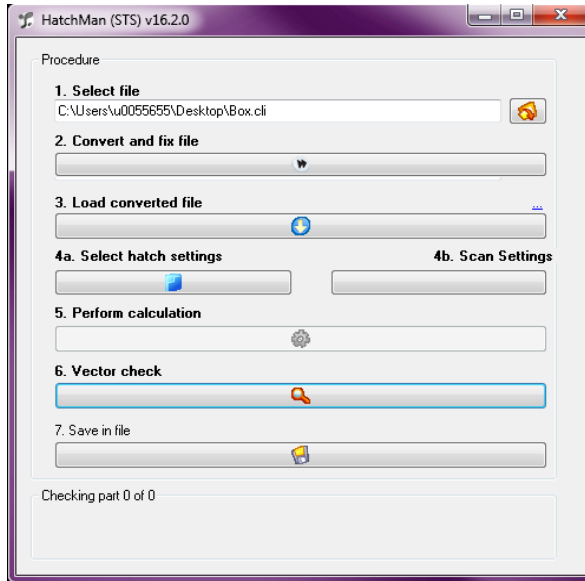


Figure A.1: The graphical user interface of *Hatchman*.

Settings

This subsection will give an overview of all the settings of *Hatchman*. These settings can be found and changed in the two pop-up windows. The first one contains mainly all the different hatching parameters. The second one is build up with some extra hatching parameters but also with some classification options to store scan vectors into the classes, to enable the classification into different heat flow situations as described in chapter 2.

Hatch settings The settings for generating the tool path can be modified in this pop-up window. All the parameters are explained shortly in this chapter. The different parameters are listed below in the same order of appearances in the pop-up window which is illustrated in *figure A.2*. A schematic representation of these parameters is illustrated in *figure A.3* to visualise all the parameters.

1. **Setting profile:** This menu allows the user to create a predefined setting profile or to load one. These setting profiles contain all the hatch settings which are listed below. This menu is added to make the program more user-friendly.

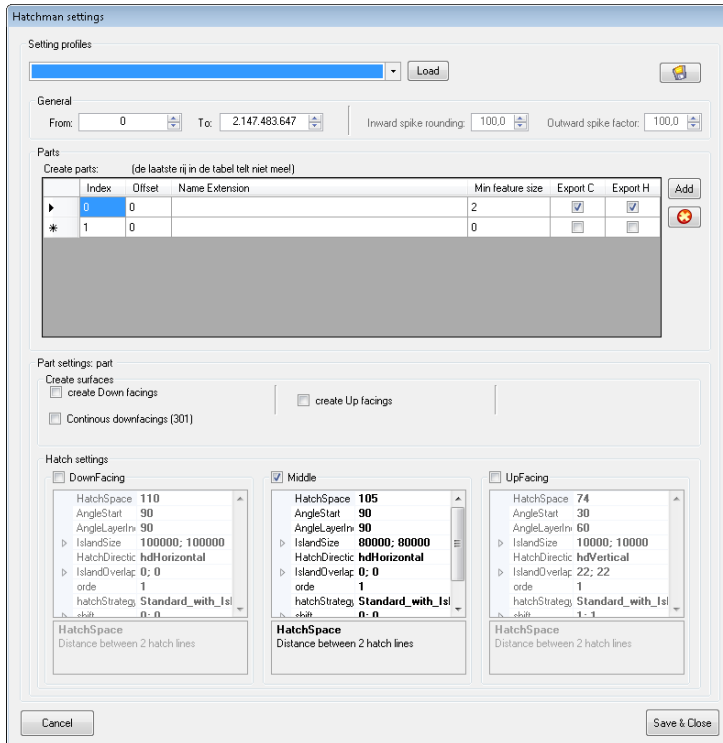


Figure A.2: A view on the pop-up window of the settings.

- General:** These general settings can be split up into two different sections. In the first section a selection of the layers that should be hatched can be made. The to hatch layers go from layer 0 till the maximum in the illustrative image. Other settings in the second section are Inward spike rounding and Outward spike rounding which define the rounding and generation of skeletons during offsetting. More information on these parameters, skeletons and roundings can be found further in this dissertation in chapter ?? Feature Optimization and details on the algorithms can be found in the paper of Moesen et al. [?].
- Parts:** In the division parts the .CLI file can be splitted into multiple parts. This can be interesting, if preferred to hatch a part multiple times with different hatch settings. By adding parts to the table sub parts are created. Each part may have a different offset (this offset is illustrated in figure A.3 as *Offset* and part settings which are described below. For

each part it is also possible to select if only the contours and/or the hatchings (fills) should be exported and stored in the .STS file.

4. **Part settings: part** These settings can be defined for each different subpart of the parts menu and contains almost all of the crucial hatching parameters (except *Offset* and the options for *Skin – Core*. All available parameters are explained below:

- **Create surfaces:** The section detects a limit amount of different zones which are necessary to classify vectors towards their heat flow conditions. The possibility is to detect down facing (on different levels) and/or up facing zones. A detailed description how this detection works is explained in the following chapter ?? Feature optimization. This detection is important to implement the methodology as described in the chapter ?? Methodology.
- **Hatch settings:** This subdivision in the Part settings contains all the parameters to generate an optimum tool path for the laser. This tool path can be different for each zone (e.g. standard fillings, up facings and/or down facings zones). The most important parameters used in this dissertation are (*figure A.3*):

Hatch space (h): Synonym for track distance; is the distance between two parallel scan vectors.

Angle start (α_0): Angle between the x-axis of the islands and of the machine in the first layer.

Angle layer increment (α_{incr}): Angle increment added for each next layer to the angle α .

Island size ($L_{island} \times W_{island}$): Containing the length and width of the generated islands.

Island overlap (O_{island}): To optimize the connection between islands an overlap is applied.

Hatch strategy: This strategy is the pattern that is used to fill the islands. *Figure A.4* shows six different patterns that are implemented in *Hatchman*. Depending on the selected hatch strategy a orde has to be given. This is necessary since fractal curves do not work with hatch spacing but with ordes. To illustrate the fractal tool paths of orde 1 and 2 are illustrated in *figure A.4*.

5.

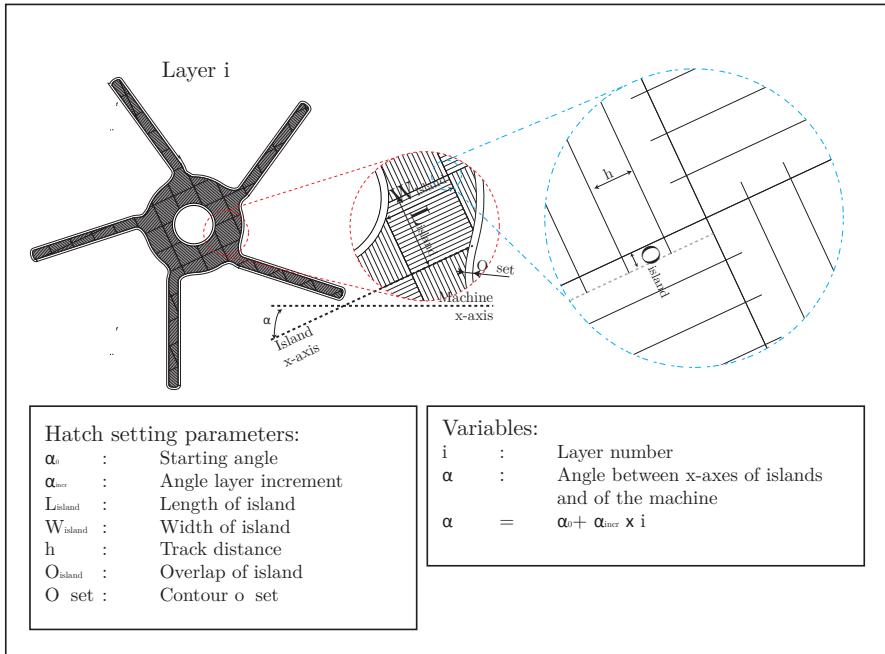


Figure A.3: A schematic overview of all the hatch settings of *Hatchman*.

Scan settings The second settings pop-up window contains all the settings for the scanning (figure A.5).

In the first section of the pop-up window the scan order can be selected. It is possible to first scan the contour and then the filling vectors or vice versa. Besides this it is possible to select a skin-core technique where you can select the amount of contours you want to scan and its offset. This is illustrated in *figure A.6*.

The second section of the scan settings pop-up window contains all the different vector classes. Each of the class can be linked to an ID number to which parameters will be linked in the machine software. By giving some classes the same ID number, the same parameters will be used for these different classes. The application of these possibilities will be illustrated in subsection.

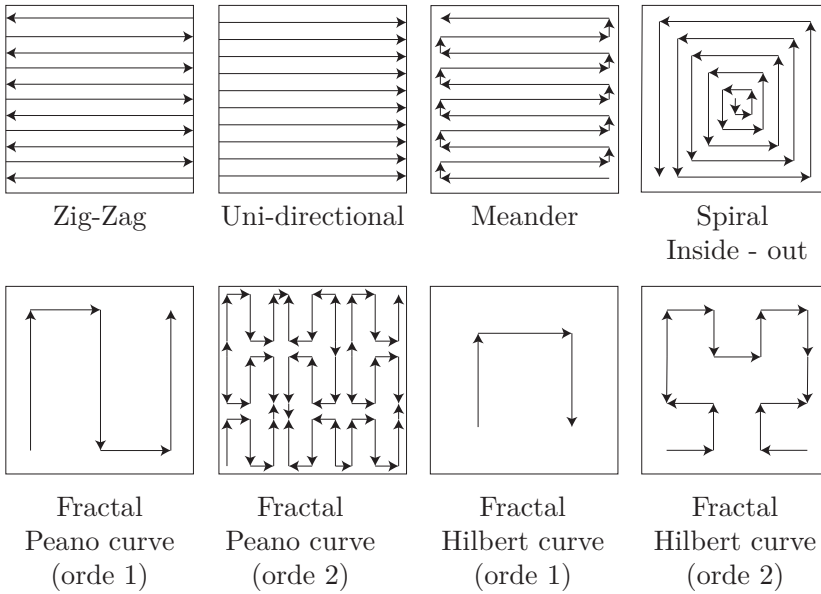


Figure A.4: Illustration of some of the different hatch strategies implemented in *Hatchman*.

Perform Calculations

Once all settings are configured and the button of perform calculations is triggered. A series of algorithms are executed for each layer. An overview of the complete sequence of algorithms is discussed in the chapter ??.

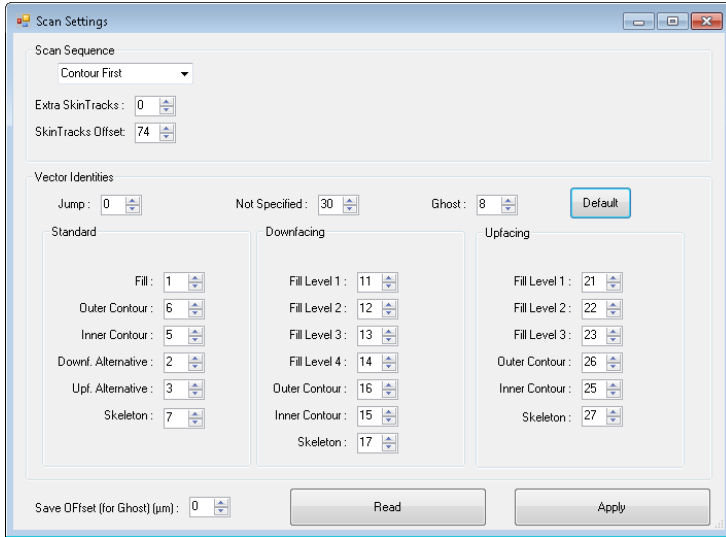


Figure A.5: The graphical user interface to select the scan settings.

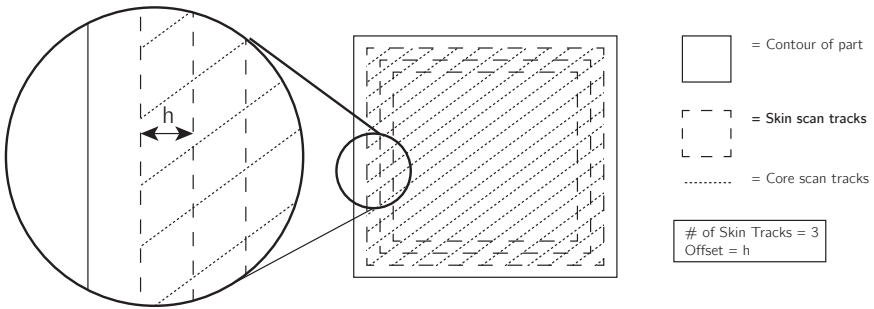


Figure A.6: A schematic overview of the Skin-Core strategy in *Hatchman*.

A.5 LabVIEW implementations

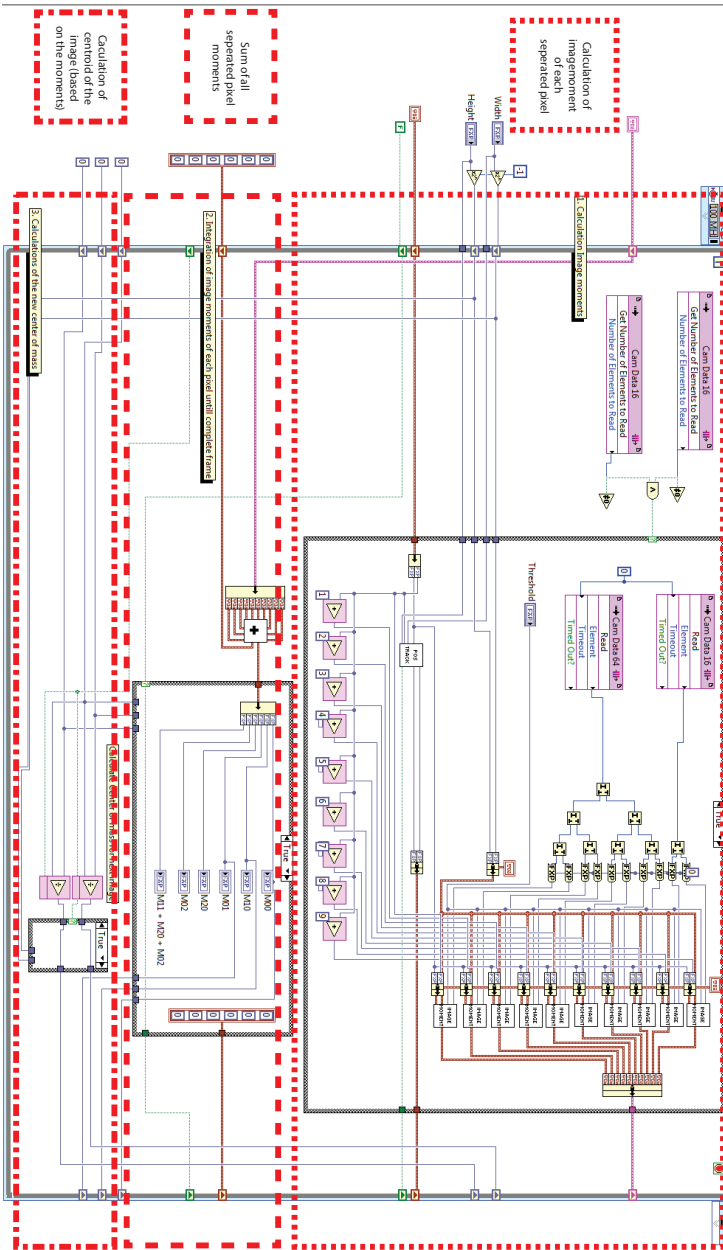


Figure A.7: The implementation of calculation of the eccentricity of the melt pool.

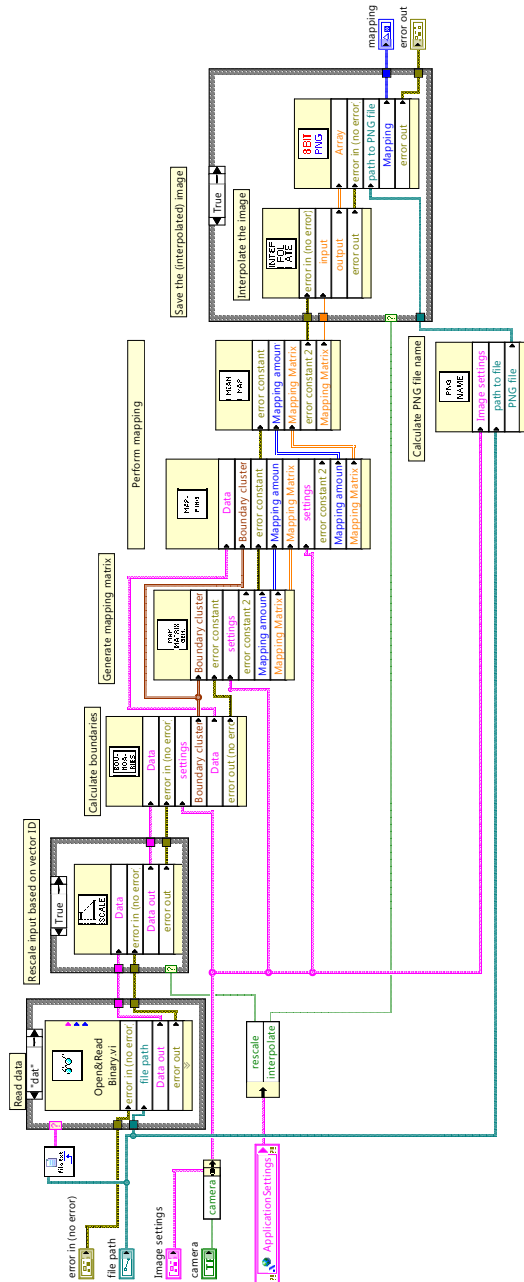


Figure A.8: Schematic overview of the *Mapping Algorithm*. [?]

FACULTY OF ENGINEERING SCIENCE
DEPARTMENT OF MECHANICAL ENGINEERING
PRODUCTION, AUTOMATION AND MACHINE DESIGN

Celestijnenlaan 300B box 2420

B-3001 Heverlee

info@mech.kuleuven.be

<http://www.mech.kuleuven.be>

